

## The application of titanium dioxide (TiO<sub>2</sub>) nanoparticles in the photo-thermal therapy of melanoma cancer model

Mohammad Ali Behnam<sup>1</sup>, Farzin Emami<sup>1</sup>, Zahra Sobhani<sup>2,3\*</sup>, Amir Reza Dehghanian<sup>4</sup>

<sup>1</sup> Nano Opto-Electronic Research Center, Electrical and Electronics Engineering Department, Shiraz University of Technology, Shiraz, Iran

<sup>2</sup> Quality Control Department, Faculty of Pharmacy, Shiraz University of Medical Sciences, Shiraz, Iran

<sup>3</sup> Pharmaceutical Sciences Research Center, Shiraz University of Medical Sciences, Shiraz, Iran

<sup>4</sup> Pathology Department, Shiraz University of Medical Sciences, Shiraz, Iran

### ARTICLE INFO

**Article type:**  
Original article

**Article history:**  
Received: Mar 4, 2018  
Accepted: Jul 16, 2018

**Keywords:**  
Hyperthermia  
Laser diode  
Melanoma cancer  
PEGylated titanium dioxide-  
(TiO<sub>2</sub>-PEG) nanoparticles

### ABSTRACT

**Objective(s):** Photo-thermal therapy (PTT) is a therapeutic method in which photon energy is converted into heat to induce hyperthermia in malignant tumor cells. In this method, energy conversion is performed by nanoparticles (NPs) to enhance induced heat efficacy. The low-cytotoxicity and high optical absorbance of NPs used in this technique are very important. In the present study, titanium dioxide (TiO<sub>2</sub>) NPs were used as agents for PTT. For increasing water dispersibility and biocompatibility, polyethylene glycol (PEG)-TiO<sub>2</sub> NPs (PEGylated TiO<sub>2</sub> NPs) were synthesized and the effect of these NPs on reducing melanoma tumor size after PTT was experimentally assessed.

**Materials and Methods:** To improve the dispersibility of TiO<sub>2</sub> NPs in water, PEG was used for wrapping the surface of TiO<sub>2</sub> NPs. The formation of a thin layer of PEG around the TiO<sub>2</sub> NPs was confirmed through thermo-gravimetric analysis and transmission electron microscopy techniques. Forty female cancerous mice were divided into four equal groups and received treatment with NPs and a laser diode ( $\lambda = 808$  nm, P = 2 W & I = 2 W/cm<sup>2</sup>) for seven min once in the period of the treatment.

**Results:** Compared to the mice receiving only the laser therapy, the average tumor size in the mice receiving TiO<sub>2</sub>-PEG NPs with laser excitation treatment sharply decreased.

**Conclusion:** The results of animal studies showed that PEGylated TiO<sub>2</sub> NPs were exceptionally potent in destroying solid tumors in the PTT technique.

### ► Please cite this article as:

Behnam MA, Emami F, Sobhani Z, Dehghanian AR. The application of titanium dioxide (TiO<sub>2</sub>) nanoparticles in the photo-thermal therapy of melanoma cancer model. Iran J Basic Med Sci 2018; 21:1133-1139. doi: 10.22038/IJBMS.2018.30284.7304

### Introduction

Cancer still remains one of the leading causes of death with increasing incidence all over the world (1). The most pervasive method of cancer treatment is chemotherapy, which normally faces the problems of drug resistance and insufficient efficacy of drug delivery into cancer cells (1, 2). Another common method in cancer treatment is surgery. Methods of cancer treatment strongly rely on tumor size, lymph node involvement, and how much the cancer has spread. Surgery in combination with chemotherapy is the primary treatment for cancers (3, 4). The advent of nanoparticles (NPs) in biomedical and bioengineering fields made a revolution in the methods of cancer therapy. Nano-scale sizes of NPs improve their ability to be attached and transported to cells (2, 5). Nano-sized particles have been used in photodynamic therapy (PDT) and sonodynamic therapy of clinical cancer studies. PDT utilizes light absorbing photosensitizers to generate highly reactive oxygen species (ROS) that can cause cell rupture. Stimulated particles could fluctuate the electrons and have them transfer their charge from a state to another one, which produces active oxygen species (6). PDT has been used to treat malignant tumors and abnormal vasculatures (7). Production of toxic singlet oxygen and high photosensitivity of treated patients in this method could limit the PDT technique (4).

Photo-thermal therapy (PTT) by means of NPs promises a new technique to efficiently treat cancer cells without any major limitation or side effects. In particular, NPs play an efficient role in converting the photon energy of laser light into heat due to their specific physicochemical properties and inducing hyperthermia in malignant tissues (2, 5). Thus far, a variety of nanostructures such as gold NPs (8), silver NPs (9), and carbon nanotubes (10) have been successfully developed in inducing hyperthermia in tumor tissues. A good candidate with specific characteristics for the PTT of tumors is titanium dioxide (TiO<sub>2</sub>) NPs.

Recently, TiO<sub>2</sub> has attracted a growing deal of interest (11, 12). It is used in pharmaceutical and cosmetic industries, and is generally considered to be biologically inert (13). It is bio-friendly and has exceptional properties, such as high refractive index, and photocatalytic and magnetic properties (14–16). Such characteristics of TiO<sub>2</sub> stem from the spontaneous formation of an oxide layer on the titanium surface (17). TiO<sub>2</sub> can destroy bacteria, viruses, fungi, and cancer cells (18) and can act as an effective catalyzer for treating malignant tumors (4, 19). PDT, drug delivery, cell imaging, biosensors for biological assay, and genetic engineering are some forms of biomedical application of TiO<sub>2</sub> NPs (5). TiO<sub>2</sub> NPs could be a good choice for

biomedical applications as agents in converting photon energy into heat in the PTT method, which is due to their super hydrophilicity (20), low-toxicity, good thermal conductivity, good optical absorption, and chemical and thermal stability *in vivo* (5). TiO<sub>2</sub> nanostructures have been used in drug delivery systems for different anti-cancer drugs, such as daunorubicin, temozolomide, doxorubicin, and cisplatin (21–23). To increase the biocompatibility of TiO<sub>2</sub> NPs, polyethylene glycol (PEG) could be attached to their surfaces. PEGylated NPs could escape the Reticulo-Endothelial System (RES) (18, 19). In the present study, TiO<sub>2</sub> NPs were evaluated as impressive agents for PTT *in vivo*. To improve the dispersibility of TiO<sub>2</sub> NPs, a layer of PEG coated the NPs. The efficacy of TiO<sub>2</sub>-PEG NPs in the treatment of melanoma cancer model in the PTT technique was also assessed.

## Materials and Methods

### Preparation and characterization of TiO<sub>2</sub>-PEG NPs

The TiO<sub>2</sub> NPs used in this study (particle size: 10–25 nm, purity: > 99%, phase: anatase) were purchased from US Research Nanomaterials, Inc., the United States. To enhance the dispersibility of the TiO<sub>2</sub> NPs in deionized water, they were coated with a layer of PEG (10). Twenty five mg TiO<sub>2</sub> NPs was suspended in 25 mL deionized water. Then, 250 mg PEG<sub>1000</sub> (Sigma-Aldrich, St. Louis, MO, the USA) was dissolved in TiO<sub>2</sub> NPs suspension. The suspension was ultrasonicated for 15 min and then stirred at room temperature overnight to allow the hydrophilic polymer to wrap around the TiO<sub>2</sub> NPs (3). After being stirred, the suspension was centrifuged at 4000 rpm for 15 min to separate the unreacted TiO<sub>2</sub> NPs, and afterward, the supernatant was collected (3, 10).

The microscopic image of the TiO<sub>2</sub>-PEG NPs was taken by a transmission electron microscope (TEM) (Philips Electron Optics, the Netherlands). The light absorption spectrum of the TiO<sub>2</sub> NPs was measured by a UV/Vis double beam spectrophotometer (PG Instruments Ltd., T80+ UV-Vis spectrophotometer, Lutterworth, the UK). Thermogravimetric analysis (TGA) was carried out by (METTLER TOLEDO, TGA<sub>2</sub>, Switzerland) under the dynamic atmosphere of an inert gas (N<sub>2</sub>) at 30 ml/min.

### Tumor induction

All experimental standards of this study were endorsed by the Animal Care and Use Committee of Shiraz University of Medical Sciences, Shiraz, Iran, and the experiments were done in accordance with the National Institutes of Health Guidelines for Care and Use of Laboratory Animals. All procedures were verified to minimize discomfort to the animals and to use as few animals as possible for statistical analysis. Fortunately, this experiment was approved by the Ethical Committee at Shiraz University of Medical Sciences.

A metastatic murine melanoma cell line, B16/F10 (NCBI C540 was purchased from the National Cell Bank of Pasteur Institute of Iran, Tehran, Iran) was cultured in an RPMI 1640 medium, under 5% CO<sub>2</sub> at the temperature of 37 °C. It was then prepared by 10 % fetal bovine serum, 100 IU/mL of penicillin and 100 µg/mL streptomycin. Forty female C57BL/6J inbred mice, weighing 25–35 g, and aged 7–9 weeks were selected for the tumor induction. The murine melanoma cells

at a number of 0.5 \* 10<sup>6</sup> were suspended in 200 µl culture medium and injected subcutaneously into the loose skin over the neck (10). The mice were housed in standard cages under standard conditions with 14:10 hr light/dark cycle (lights on at 6:00 a.m.), at an ambient temperature of 25 ± 2 °C and 30% relative humidity. They were randomly divided into four equal independent groups (N = 10) and had access to normal chow and water *ad libitum*. Melanoma is a superficial tumor, so its changes could be observed easily during the treatment.

### Photo-thermal therapy of tumors

Two weeks after the injection of the murine melanoma cell line, the melanoma tumors had sufficiently grown (approximately 1 cm<sup>3</sup>) to start the treatment. The animals were anesthetized by injecting Ketamine and Xylazine intramuscularly (IM). The tumor regions were shaved and measured by a caliper and an ultrasound machine (Ultrasonix SonixOP; Burnaby, BC, Canada). The tumor size was estimated through the following equation:

$$\text{Tumor volume} = (L/2) * W^2 \text{ (mm}^3\text{)} \text{ (3, 10)}$$

In this equation, L and W indicate the length and width of the tumor, respectively. The treatment started according to the following grouping:-

Group I (TiO<sub>2</sub>+laser): 200 µl/cm<sup>3</sup> (tumor volume) TiO<sub>2</sub>-PEG NPs (1 mg/ml) were injected directly into the tumor and then excited by a laser diode.

Group II (Laser therapy): The laser therapy was done without any pre-treatment with the NPs.

Group III (TiO<sub>2</sub> NPs): 200 µl/cm<sup>3</sup> (tumor volume) TiO<sub>2</sub>-PEG NPs (1 mg/ml) were injected directly into the tumor without any laser excitation.

Group IV (Control): This group did not receive any treatment.

Groups I and II were irradiated by a continuous wave (CW) near-infrared (NIR) laser diode (DAJCO, Shiraz, Iran) with these specifications: wavelength = 808 nm; power = 2 W; spot size = 1 cm<sup>2</sup>; and intensity = 2 W/cm<sup>2</sup> for seven min once in the period of the treatment (10, 24). However, the control cases were not irradiated. The tumor sizes were measured three days after the laser excitation. After the period of the treatment, the animals were euthanized and their masses were excised for histopathologic examination (five cases of TiO<sub>2</sub>+laser group were euthanized after three months of follow-up).

### Histopathological examination

The specimens were treated, formalin fixed paraffin embedded (FFPE) blocks were provided, and the slides were stained with Hematoxylin and Eosin (H&E) method. The specimens were sampled for microscopy evaluation.

### Statistical analysis

The numerical results of this study were presented as mean ± standard deviation (SD). The normality of the results was analyzed by the one-sample Kolmogorov-Smirnov test. Significant differences between the values were statistically tested by Student's t-test in each group. Multiple comparisons at multiple time points were tested by ANOVA with Repeated Measures. The statistical analyses were performed using SPSS®

statistical software for Windows®, version 20.0 (SPSS Inc., Chicago, IL, USA). A *P*-value of < 0.05 was regarded as significant.

## Results

### Preparation and characterization of the TiO<sub>2</sub>-PEG NPs

Figure 1 shows the TEM image of PEG-coated TiO<sub>2</sub> NPs. Accordingly, a continuous layer of PEG with the average thickness of a few nanometers was formed on the surface of the TiO<sub>2</sub> NPs.

The UV-Vis light absorption spectrum of the TiO<sub>2</sub>-PEG NPs is provided in Figure 2. As shown in this figure, absorption occurred in two regions. It reached a peak at the UV range, and then it gradually reduced at visible-near-IR range. Despite being at the wavelength of 808 nm, photoabsorption of these NPs is relatively low compared to those with a UV wavelength, but due to the deep penetration of NIR wavelength into the body (25), a CW NIR laser diode (808 nm) was used for photo irradiation (10). Additionally, the UV range is dangerous to the body and may cause gene mutation and DNA damage (26).

The TGA measurements provided further evidence regarding the interaction between the PEG and the surfaces of the TiO<sub>2</sub> NPs. Figure 3 shows the thermogram of the physical mixture of the TiO<sub>2</sub> NPs and PEG, and also the thermo-gram of TiO<sub>2</sub>-PEG. In the physical mixture of the TiO<sub>2</sub> NPs and PEG, weight loss occurred at two stages, 224.16 °C and 299.26 °C. TiO<sub>2</sub>-PEG showed a completely different pattern in comparison with the physical mixture of the TiO<sub>2</sub> NPs and PEG. In the TiO<sub>2</sub>-PEG pattern, weight loss occurred at one stage at 312.93 °C.

### Photo-thermal therapy of tumors

The tumor sizes were recorded three days after laser excitation. The tumor sizes of different groups (before and three days after the treatment with PTT) were analyzed and the results showed significant differences between groups I, III, and IV (*P*-value<0.05).

The decrease in tumor volume in group I is obvious as indicated in Figure 4. As can be seen in Figure 4, the average tumor volume in the Control and TiO<sub>2</sub> NPs groups increased. However, it significantly decreased in the TiO<sub>2</sub>+laser group. The tumor sizes in the Laser therapy group were not significantly different during the treatment, but the tumors ceased to grow further. The slopes of tumor size against time in the Control, Laser therapy, TiO<sub>2</sub>+laser, and TiO<sub>2</sub> NPs groups were about +103.58 mm<sup>3</sup>/days, +19.07 mm<sup>3</sup>/days, -40.60 mm<sup>3</sup>/days, and +86.70 mm<sup>3</sup>/days, respectively (“+” indicates increase and “-” indicates a decrease in tumor size).

The histopathologic evaluation of the tumors indicates a severe necrosis in the TiO<sub>2</sub>+laser group. Necrosis was the most important discriminator among the cases and its percentage was higher in the TiO<sub>2</sub>+laser group compared to the Laser therapy, TiO<sub>2</sub>, and Control groups, which indicates the noticeable effect of the TiO<sub>2</sub>-PEG NPs in inducing hyperthermia in the tumors when excited with a laser diode. Regressive fibrosis, lymphocytic infiltration, vascular invasion, or neurotropism were not seen in the cases. The histopathologic results are shown in Table 1 and Figure 6.

Five cases in the TiO<sub>2</sub>+laser group were followed up for three months after the treatment to analyze the trend

of tissue regeneration. The stages of tumor treatment are shown in Figure 7, which indicates that the hair color of the tumor region changed after three months.

For further examination, three months after the start of the treatment these cases were euthanized and their mass was formalin fixed and sent for histopathologic evaluation. As shown in Figure 8, histopathology of the skin, the soft tissue of the back, and the bone marrow of the treated cases showed that there was no evidence of melanoma cancer in TiO<sub>2</sub>+laser cases after three months of follow-up.

## Discussion

Titanium dioxide NPs have a wide variety of applications in medicine and life sciences. These NPs can be used as a carrier for drugs especially anti-cancer drugs and as an agent for photo-dynamic or PTT of solid tumors. TiO<sub>2</sub> NPs have been used as drug delivery systems for different anti-cancer drugs, such as paclitaxel, doxorubicin, daunorubicin, temozolomide, and camptothecin (18, 27–30). In these studies, anti-tumor efficiency could be improved by TiO<sub>2</sub> NPs. However, these NPs tend to aggregate in aqueous media and may cause problems in biological systems. In order to prevent the aggregation of these NPs, their surfaces should be modified. One of the most common methods to prevent aggregation of NPs is to cover them with hydrophilic polymers (31). PEG is one of the best polymers to solve this problem. Through attachment of PEG to the surface of the NPs, the biocompatibility of the NPs would be increased. In addition, PEGylated NPs evade the RES (18). Formation of a thin layer of polymer on the surface of TiO<sub>2</sub> NPs through a simple adsorption method is reported in some studies (18, 32, 33). We used this polymer to improve the water dispersibility of TiO<sub>2</sub> NPs. The TEM and TGA techniques indicated the formation of a thin layer around the NPs. Then, these prepared NPs were used for PTT of solid melanoma.

The photobiological effects of visible and NIR light rely on their wavelengths and could be affected by the structure, vasculature, thickness, and pigmentation of the skin's strata (34, 35). It is reported that a polarized beam in the visible-NIR range can cause biological effects in cells through electron oscillation inducement (36). Optical radiation with a longer wavelength penetrates further into the body than a shorter one (25, 37). Visible light is widely absorbed by hemoglobin of the vasculature and the melanin located in the skin (37, 38). Infrared beam affects the body through transferring thermal energy into tissues. In the infrared spectrum, scattering increases largely in the body component ; therefore, light will penetrate deeply into the body (34, 39). NIR beam deeply penetrates into tissues and can be effectively utilized in cancer treatment. Some nano-structures, such as plasmonic NPs (40) and CNTs (10), can absorb NIR light and effectively convert its energy into heat. The stimulation of NPs causes vibrational stress of electrons and makes them transmit from the ground states to the excited states. The energy caused by electrons' displacement is converted into heat by electron-electron relaxation and electron-photon relaxation (40, 41).

Stimulation of TiO<sub>2</sub> NPs with electromagnetic radiation in the range of visible or NIR light causes

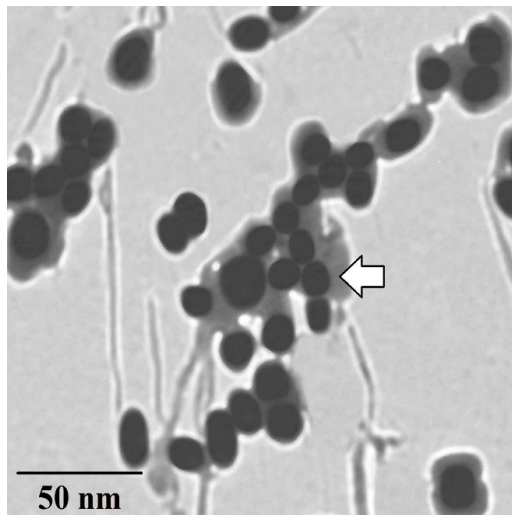


**Figure 1.** The TEM image of the TiO<sub>2</sub>-PEG NPs; a layer of PEG was formed on the surface of the TiO<sub>2</sub> nanospheres (the arrow shows the PEG layer around the TiO<sub>2</sub> NPs)

generation of cytotoxic ROS that induce apoptosis along with increasing the tumor region temperature (42, 43). These effects are the principles of PDT and PTT, respectively.

Many researchers showed phototoxic effect of TiO<sub>2</sub> NPs after UV-A radiation on a series of cancer cell lines such as cervical cancer cells (HeLa), bladder cancer cells (T24), monocytic leukemia cells (U937), adenocarcinoma cells (SPC-A1), colon carcinoma cells (Ls-174-t), breast epithelial cancer cells (MCF-7, MDA-MB-468), glioma cells (U87), and human hepatoma cells (Bel 7402) (5).

Penetration of the UV-A spectrum in the body is too low. Besides, the UV-A spectrum could have an adverse effect on biological molecules. Therefore, we used NIR wavelength for tumor ablation. NIR wavelength is more transmissive through the body and has low attenuation in biological systems (44, 45). Wenjun Ni *et al.* showed that black TiO<sub>2</sub> NPs are efficient as photosensitizers for PDT to kill bladder cancer cells. They used 808 nm light for irradiation of black TiO<sub>2</sub> NPs (46). In reported studies, the efficacy of TiO<sub>2</sub> NPs after UV and NIR irradiation on the cancer cells was evaluated in the *in vitro* cell culture medium (32, 47). Considering these studies, we

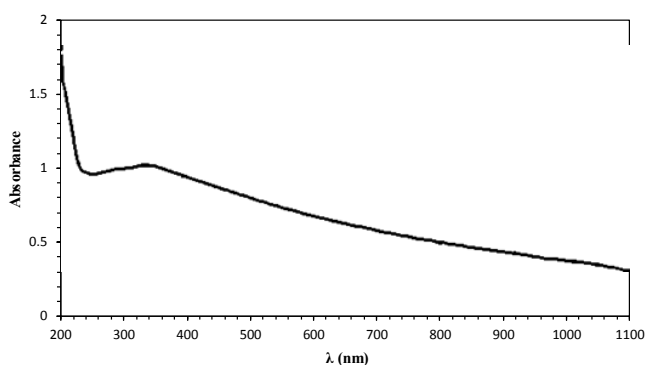


**Figure 2.** The UV-Vis light absorption spectrum of the TiO<sub>2</sub>-PEG NPs; absorption happened in two regions. It reached a peak at UV range, then gradually reduced at visible-near-IR range

**Table 1.** Histopathologic results of tumor tissues after treatment in different groups

Groups	Necrosis (%)	Breslow's thickness	Tumor stage after the treatment according to AJCC 2010
TiO <sub>2</sub> +laser	(0.70±0.05)*100	>4mm	IIA
Laser therapy	(0.25±0.03)*100	>4mm	IIB
TiO <sub>2</sub> NPs	< (0.05±0.01)*100	>4mm	IIB
Control	< (0.05±0.01)*100	>4mm	IIB

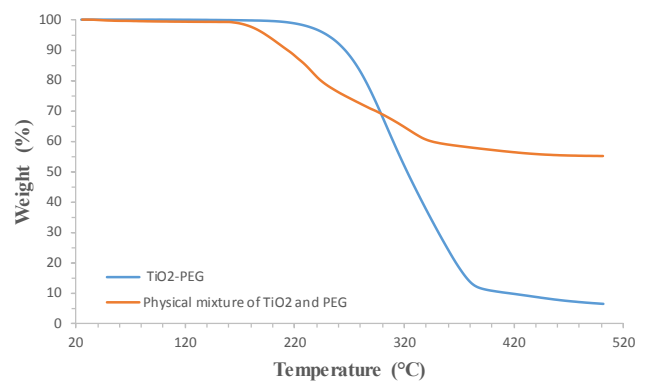


**Figure 3.** The thermo-grams of the physical mixture of the TiO<sub>2</sub> NPs and PEG, and also synthesized TiO<sub>2</sub>-PEG; precisely, in the physical mixture of the TiO<sub>2</sub> NPs and PEG, weight loss appeared at two stages: 224.16 °C and 299.26 °C. TiO<sub>2</sub>-PEG showed a completely different pattern

performed our research in the *in vivo* melanoma tumor model. In order to assess the PTT effects of the TiO<sub>2</sub>-PEG NPs, after injection of the TiO<sub>2</sub>-PEG NPs into the tumor, tumor sites were irradiated by an 808 CW laser diode. Results showed that the localized NPs caused significant necrosis due to the deep penetration of NIR beam into the body and good photoabsorption of TiO<sub>2</sub>-PEG at the wavelength of 808 nm. The findings of the animal studies indicated that in the TiO<sub>2</sub>+laser group, not only did the tumor growth cease, but the tumor size also shrank. The

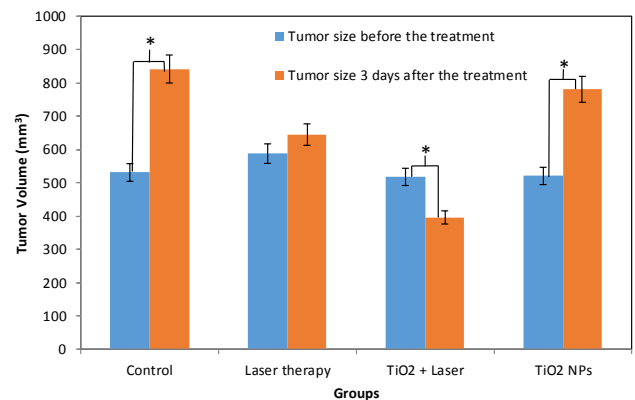


**Figure 4.** The tumor volume of different cases before and three days after PTT (\* shows statistically significant difference ( $P < 0.05$ )); the average tumor volume increased in the Control, TiO<sub>2</sub> NPs, and Laser therapy groups, but it decreased in the TiO<sub>2</sub>+laser group

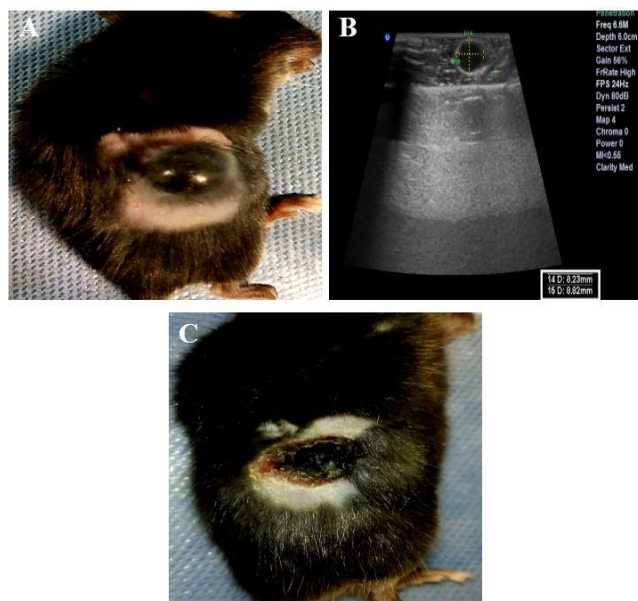


**Figure 5.** Tumor ablation stages in the TiO<sub>2</sub>+laser group with the PTT technique. (A, B): the photograph and the ultrasonography image of a cancerous mouse in the TiO<sub>2</sub>+laser group before the treatment, respectively. (C): the photograph of the mouse three days after the treatment (sonography was not feasible)

histopathological examination showed 70% necrosis in the TiO<sub>2</sub>+laser group, which confirms the good efficiency of the TiO<sub>2</sub>-PEG NPs in the NIR spectrum for the PTT method. Furthermore, following up the TiO<sub>2</sub>+laser cases for three months demonstrates good biocompatibility of these NPs in this technique.

This reported application of the TiO<sub>2</sub>-PEG NPs for *in vivo* trials could promise a biocompatible agent for this cancer therapy technique. Considering the results, the next step is to assess the efficacy of the TiO<sub>2</sub> NPs in tumor suppression by hyperthermia therapy and to deliver anti-cancer drugs to tumor sites, concurrently.

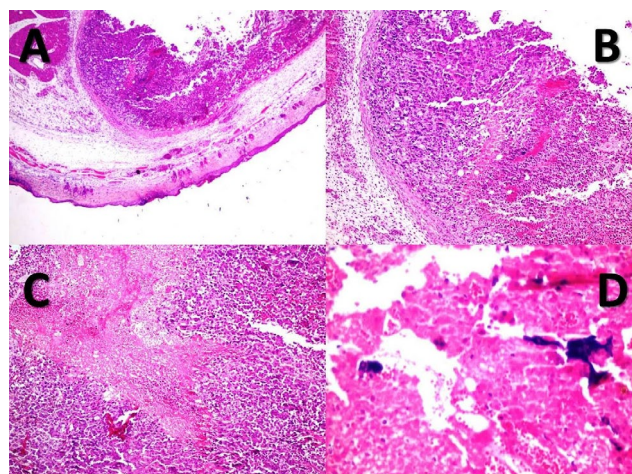


**Figure 6.** Nodular melanoma with a central necrosis in the TiO<sub>2</sub>+laser group. (A, B, C): histopathology of the skin (X40, H&E (A)), (X100, H&E (B, C)). (D): TiO<sub>2</sub>-PEG NPs present in the necrotic areas (X400, H&E). Accordingly, a severe necrosis was seen in the TiO<sub>2</sub>+laser group

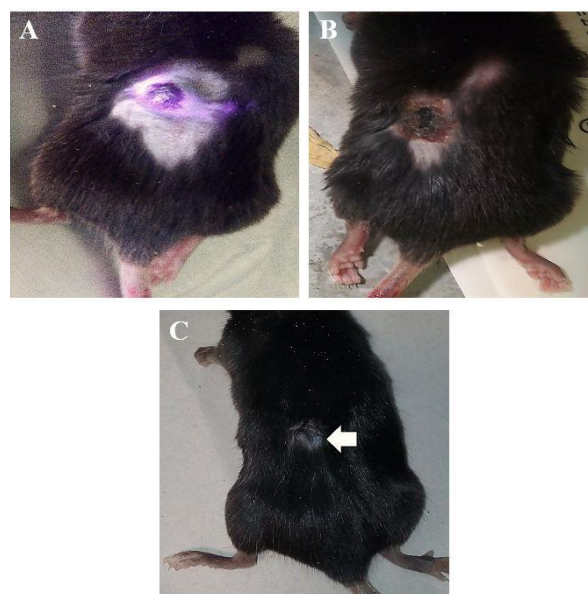


**Figure 7.** Three months of follow-up in the TiO<sub>2</sub>+laser cases treated with PTT. (A, B, C): before, three days, and three months after the treatment, respectively (the arrow indicates the changes of hair color in the tumor site after three months)

## Conclusion

The present study assessed the application of PEGylated TiO<sub>2</sub> NPs in inducing hyperthermia and necrosis in malignant tumor cells for the PTT technique. The animal trials in this study confirmed the relatively high efficacy of such NPs in destroying solid tumors without any symptom of cancer cells in treated cases. Therefore, the TiO<sub>2</sub>-PEG NPs could be utilized as a potent agent with low toxicity in the PTT technique for ablating solid tumors.

## Acknowledgment

This work was financially supported by Shiraz

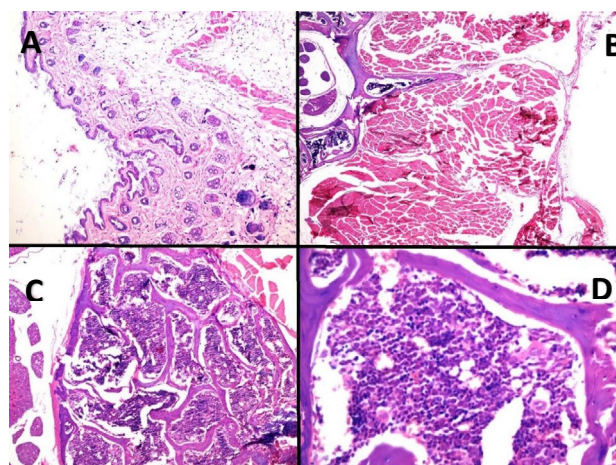


**Figure 8.** The histopathology of the treated cases in the TiO<sub>2</sub>+Laser group after three months of follow-up. (A): the histopathology of the skin shows no residue of the tumor and scar formation (X40, H&E). (B): the histopathology of the soft tissue of the back shows no evidence of tumor residue (X40). (C, D): the histopathology of the bone marrow shows normocellular marrow with polymorphic presence of hematopoietic cells (X40, X400)

University of Medical Sciences, Shiraz, Iran as a research project (approval no. 12079). We would like to especially thank Dr. Ali Mashreghi, a faculty member of Materials Science and Engineering Department, Shiraz University of Technology, Shiraz, Iran and Dr. Mohammad Hosein Bagheri, Doctor of Veterinary Medicine, Shiraz University, Shiraz, Iran.

### Conflicts of Interest

The authors declare that they have no conflicts of interest. Authors disclose all relationships or interests that could have direct or potential influence or impart bias on the work.

### References

- Ortiz R, Melguizo C, Prados J, Alvarez PJ, Caba O, Rodriguez-Serrano F, *et al.* New gene therapy strategies for cancer treatment: a review of recent patents. *Recent Pat Anticancer Drug Discov* 2012; 7:297-312.
- Bertrand N, Leroux J-CC. The journey of a drug-carrier in the body: an anatomo-physiological perspective. *J Control Release* 2012; 161:152-163.
- Behnam MA, Emami F, Sobhani Z, Koohi-Hosseiniabadi O, Dehghanian AR, Zebarjad SM, *et al.* Novel combination of silver nanoparticles and carbon nanotubes for plasmonic photo thermal therapy in melanoma cancer model. *Adv Pharm Bull* 2018; 8:49-55.
- Moosavi Nejad S, Takahashi H, Hosseini H, Watanabe A, Endo H, Narihira K, *et al.* Acute effects of sono-activated photocatalytic titanium dioxide nanoparticles on oral squamous cell carcinoma. *Ultrason Sonochem* 2016; 32:95-101.
- Yin ZF, Wu L, Yang HG, Su YH. Recent progress in biomedical applications of titanium dioxide. *Phys Chem Chem Phys* 2013; 15:4844-4858.
- Bibin AB, Kume K, Tsutumi K, Fukunaga Y, Ito S, Imamura Y, *et al.* Observation the distribution of titanium dioxide nano-particles in an experimental tumor tissue by a raman microscope. *AIP Conf Proc* 2011; 55-58.
- Uehara M, Ikeda H, Nonaka M, Sumita Y, Nanashima A, Nonaka T, *et al.* Predictive factor for photodynamic therapy effects on oral squamous cell carcinoma and oral epithelial dysplasia. *Arch Oral Biol* 2011; 56:1366-1372.
- Yakunin AN, Avetisyan Y, Tuchin VV. Quantification of laser local hyperthermia induced by gold plasmonic nanoparticles. *J Biomed Opt* 2015; 20:51030-51030.
- Thompson EA, Graham E, Macneill CM, Young M, Donati G, Wailes EM, *et al.* Differential response of MCF7, MDA-MB-231, and MCF 10A cells to hyperthermia, silver nanoparticles and silver nanoparticle-induced photothermal therapy. *Int J Hyperthermia* 2014; 30:312-323.
- Sobhani Z, Behnam MA, Emami F, Dehghanian A, Jamhiri I. Photothermal therapy of melanoma tumor using multiwalled carbon nanotubes. *Int J Nanomedicine* 2017; 12:4509-4517.
- Jhuang YY, Cheng WT. Fabrication and characterization of silver/titanium dioxide composite nanoparticles in ethylene glycol with alkaline solution through sonochemical process. *Ultrason Sonochem* 2016; 28:327-333.
- Eskandarloo H, Badieli A, Behnajady MA, Ziarani GM. Ultrasonic-assisted sol-gel synthesis of samarium, cerium co-doped TiO<sub>2</sub> nanoparticles with enhanced sonocatalytic efficiency. *Ultrason Sonochem* 2015; 26:281-292.
- Jugan ML, Barillet S, Simon-Deckers A, Sauvaigo S, Douki T, Herlin N, *et al.* Cytotoxic and genotoxic impact of TiO<sub>2</sub> nanoparticles on A549 cells. *J Biomed Nanotechnol* 2011; 7:22-23.
- Carp O, Huisman CL, Reller A. Photoinduced reactivity of titanium dioxide. *Prog Solid State Chem* 2004; 32:33-177.
- Haseeb A, Hasan MM, Masjuki HH. Structural and mechanical properties of nanostructured TiO<sub>2</sub> thin films deposited by RF sputtering. *Surf Coat Technol* 2010; 205:338-344.
- He Q, Wen X, Ma P, Deng X. Alkali induced morphology and property improvements of TiO<sub>2</sub> by hydrothermal treatment. *J Wuhan University Tech-Mater. Sci. Ed* 2008; 23:503-506.
- Tanner K E. Titanium in medicine. *Proc Inst Mech Eng H* 2016; 216:215-215.
- Devanand Venkatasubbu G, Ramasamy S, Ramakrishnan V, Kumar J. Folate targeted PEGylated titanium dioxide nanoparticles as a nanocarrier for targeted paclitaxel drug delivery. *Adv Powder Technol* 2013; 24:947-954.
- Yamaguchi S, Kobayashi H, Narita T, Kanehira K, Sonezaki S, Kudo N, *et al.* Sonodynamic therapy using water-dispersed TiO<sub>2</sub>-polyethylene glycol compound on glioma cells: comparison of cytotoxic mechanism with photodynamic therapy. *Ultrason Sonochem* 2011; 18:1197-1204.
- Wang R, Hashimoto K, Fujishima A, Chikuni M, Kojima E, Kitamura A, *et al.* Light-induced amphiphilic surfaces. *Nature* 1997; 388:431-432.
- Xu P, Wang R, Ouyang J, Chen B. A new strategy for TiO<sub>2</sub> whiskers mediated multi-mode cancer treatment. *Nanoscale Res Lett* 2015; 10:94-104.
- Ren W, Zeng L, Shen Z, Xiang L, Gong A, Zhang J, *et al.* Enhanced doxorubicin transport to multidrug resistant breast cancer cells via TiO<sub>2</sub> nanocarriers. *RSC Adv* 2013; 3:20855-20855.
- Liu E, Zhou Y, Liu Z, Li J, Zhang D, Chen J, *et al.* Cisplatin loaded hyaluronic acid modified TiO<sub>2</sub> nanoparticles for neoadjuvant chemotherapy of ovarian cancer. *J Nanomater* 2015; 2015:1-8.
- Zhang Z, Wang J, Nie X, Wen T, Ji Y, Wu X, *et al.* Near infrared laser-induced targeted cancer therapy using thermoresponsive polymer encapsulated gold nanorods. *J Am Chem Soc* 2014; 136:7317-7326.
- Brownell J, Wang S, Tsoukas MM. Phototherapy in cosmetic dermatology. *Clin Dermatol* 2016; 34:623-627.
- Narayanan DL, Saladi RN, Fox JL. Review: ultraviolet radiation and skin cancer. *Int J Dermatol* 2010; 49:978-986.
- Jiao Z, Chen Y, Wan Y, Zhang H. Anticancer efficacy enhancement and attenuation of side effects of doxorubicin with titanium dioxide nanoparticles. *Int J Nanomedicine* 2011; 6:2321-2326.
- Li Q, Wang X, Lu X, Tian H, Jiang H, Lv G, *et al.* The incorporation of daunorubicin in cancer cells through the use of titanium dioxide whiskers. *Biomaterials* 2009; 30:4708-4715.
- López T, Sotelo J, Navarrete J, Ascencio JA. Synthesis of TiO<sub>2</sub> nanostructured reservoir with temozolomide: structural evolution of the occluded drug. *Opt Mater* 2006; 29:88-94.
- Kim C, Kim S, Oh WK, Choi M, Jang J. Efficient intracellular delivery of camptothecin by silica/titania hollow nanoparticles. *Chemistry* 2012; 18:4902-4908.
- Mano SS, Kanehira K, Sonezaki S, Taniguchi A. Effect of polyethylene glycol modification of TiO<sub>2</sub> nanoparticles on cytotoxicity and gene expressions in human cell lines. *Int J Mol Sci* 2012; 13:3703-3717.
- Naghbi S, Madaah Hosseini HR, Faghihi Sani MA, Shokrgozar MA, Mehrjoo M. Mortality response of folate receptor-activated, PEG-functionalized TiO<sub>2</sub> nanoparticles for doxorubicin loading with and without ultraviolet irradiation. *Ceram Int* 2014; 40:5481-5488.
- Du Y, Ren W, Li Y, Zhang Q, Zeng L, Chi C, *et al.* The enhanced chemotherapeutic effects of doxorubicin loaded PEG coated

- TiO<sub>2</sub> nanocarriers in an orthotopic breast tumor bearing mouse model. *J Mater Chem B* 2015; 3:1518–1528.
34. Sowa P, Rutkowska-Talipska J, Sulkowska U, Rutkowski K, Rutkowski R. Electromagnetic radiation in modern medicine: physical and biophysical properties. *Ann Med* 2012; 19:139–142.
35. Sowa P, Rutkowska-Talipska J, Rutkowski K, Kosztyła-Hojna B, Rutkowski R. Optical radiation in modern medicine. *Postepy Dermatol Alergol* 2013; 30:246–251.
36. Penjweini R, Mokmeli S, Becker K, Dodt H-U, Saghafi S. Effects of UV-, visible-, near-infrared beams in three therapy resistance case studies of fungal skin infections. *Optics Photonics J* 2013; 3:1–10.
37. Bashkatov AN, Genina EA, Tuchin V V. Optical properties of skin, subcutaneous, and muscle tissues: a review. *J Innov Opt Health Sci* 2011; 4:9–38.
38. Juzeniene A, Brekke P, Dahlback A, Andersson-Engels S, Reichrath J, Moan K, *et al.* Solar radiation and human health. *Rep Prog Phys* 2011; 74:66701–66757.
39. Polefka TG, Meyer T a, Agin PP, Bianchini RJ. Effects of solar radiation on the skin. *J Cosmet Dermatol* 2012; 11:134–143.
40. Huang X, El-Sayed M a. Plasmonic photo-thermal therapy (PPTT). *Alexandria J Med* 2011; 47:1–9.
41. Huang X, El-Sayed M a. Gold nanoparticles: optical properties and implementations in cancer diagnosis and photothermal therapy. *J Adv Res* 2010; 1:13–28.
42. Vinardell M, Mitjans M. Antitumor activities of metal oxide nanoparticles. *Nanomaterials* 2015; 5:1004–1021.
43. Kwatra D, Venugopal A, Anant S. Nanoparticles in radiation therapy: a summary of various approaches to enhance radiosensitization in cancer. *Transl Cancer Res* 2013; 2:330–342.
44. Filonov GS, Piatkevich KD, Ting L-MM, Zhang J, Kim K, Verkhusha VV. Bright and stable near-infrared fluorescent protein for *in vivo* imaging. *Nat Biotechnol* 2011; 29:757–761.
45. Shcherbakova DM, Verkhusha VV. Near-infrared fluorescent proteins for multicolor *in vivo* imaging. *Nat Methods* 2013; 10:751–754.
46. Ni W, Li M, Cui J, Xing Z, Li Z, Wu X, *et al.* 808 nm light triggered black TiO<sub>2</sub> nanoparticles for killing of bladder cancer cells. *Mater Sci Eng C Mater Biol Appl* 2017; 81:252–260.
47. Petković J, Kuzma T, Rade K, Novak S, Filipič M. Pre-irradiation of anatase TiO<sub>2</sub> particles with UV enhances their cytotoxic and genotoxic potential in human hepatoma HepG2 cells. *J Hazard Mater* 2011; 196:145–152.